3-DIMENSIONAL STUDY OF NONLINEAR BEHAVIOR OF REINFORCED CONCRETE COLUMN UNDER REPEATED LATERAL FORCES

by

Tadashi Sugano[I], Takashi Miyashita[II], Norio Inoue[II]

SUMMARY

The nonlinear behavior of reinforced concrete columns subjected to earthquake loads is studied by the 3-dimensional Finite Element Method which enables dealing with repeated reversal loads. For the yielding criteria of concrete, Drucker-Prager's function is assumed which can introduce the confinement effect by considering the bulk expansion. In the beginning experiments and their simulation analyses of columns subjected to axial force only was conducted to establish the nonlinear parameter of concrete. Then a simulation analysis of a hooped column subjected to repeated lateral forces and axial force was conducted. This pursued the reversal of loading from the positive to the negative region.

INTRODUCTION

When a reinforced concrete column is subjected to repeated lateral forces, such as earthquake loads, its plastic behavior is considerably influenced not only by logitudinal reinforcement but also by lateral reinforcement, which confines core concrete. This paper presents a study of the three dimensional nonlinear behavior of reinforced concrete columns by experiements and analyses, with attention given to afore-mentioned confining effect.

METHOD OF ANALYSIS

A reinforced concrete column is considered to be composed of core concrete, cover concrete, longitudinal and lateral reinforcing bars, and bond between concrete and reinforcing bars as shown in Fig. 1 (1, 2, 4, 5).

Modeling of Core Concrete Element

A core concrete is represented by a hexahedral isoparametric element (7). The nonlinearity of concrete is judged by the stress and strain at eight Gaussian points respectively.

1) Compressive Side

The hysteretic loop of concrete is defined as the tri-linear curve which is expressed under uniaxial force (Fig. 2). Below the first yielding point the concrete remains elastic and after that it is semi-elastic up to the second yielding point. After the second point the strength is constant and crush occurs when the strain reaches the limit value, where the sustained forces are released. In reversal region the usual tri-linear rule is adopted.

I. Dr. Eng., Senior Research Eng., Muto Institute of Kajima Corp., Tokyo, Japan
II. Senior Research Eng., Muto Institute of Kajima Corp., Tokyo, Japan

In tri-axial field the constitutive equation of concrete is defined by the initial yield condition, flow rule and hardening rule indicated below. The constants adopted in their rules are established to be adequate to uni-axial condition. Then the first yield surface and the second one are considered homologous and the ultimate strain is replaced with the ultimate equivalent plastic strain.

Initial Yield Condition: For the yielding criteria of concrete, Drucker-Prager's function is adopted which can introduce the bulk expansion caused by the plastic deformation of concrete,

$$f = \frac{3}{2}\alpha(\sigma_x+\sigma_y+\sigma_z)+f_0 = k \tag{1}$$

$$f_0^2 = \frac{1}{2}\{(\sigma_y-\sigma_z)^2+(\sigma_z-\sigma_x)^2+(\sigma_x-\sigma_y)^2+6(\tau_{yz}^2+\tau_{zx}^2+\tau_{xy}^2)\} \tag{2}$$

where α and k are constants. This yield function can be shown by principal stress field as in Fig. 3.

Flow Rule: Due to v. Mises the plastic strain increment vector $\{d\varepsilon^p\}$ lies in the exterior normal of the yield surface at the stress point (Fig. 4).

$$\{d\varepsilon^p\} = \left\{\frac{\partial f}{\partial \sigma}\right\} d\lambda \qquad d\lambda > 0 \tag{3}$$

Hardening Rule: Prager's kinematic hardening rule modified by Ziegler (6) is used (Fig. 5). The incremental translation of the center of the yield surface $\{d\sigma_0\}$ is defined by

$$\{d\sigma_0\} = \{\sigma-\sigma_0\}\, d\mu \qquad d\mu > 0 \tag{4}$$

Here the yield surface moves in the direction of the vector CP connecting the center of the yield surface with the stress point. The scalar $d\mu$ in Eq. 4 is determined by the condition that P remains on the yield surface in plastic flow. This condition is

$$\{d\sigma-d\sigma_0\}^T\left\{\frac{\partial f}{\partial \sigma}\right\} = 0 \tag{5}$$

and from Eq. 4 and Eq. 5 the following is obtained.

$$d\mu = \frac{\left\{\frac{\partial f}{\partial \sigma}\right\}^T\{d\sigma\}}{\{\sigma-\sigma_0\}^T\left\{\frac{\partial f}{\partial \sigma}\right\}} \tag{6}$$

If it is assumed that the vector $c\{d\varepsilon^p\}$ is the projection of $\{d\sigma\}$ (and thus of $\{d\sigma_0\}$) on the exterior normal of the yield surface, this condition is

$$\{d\sigma-c\,d\varepsilon^p\}^T\left\{\frac{\partial f}{\partial \sigma}\right\} = 0 \tag{7}$$

then from Eq. 3 and Eq. 7 the following is obtained.

$$d\lambda = \frac{1}{c}\frac{\left\{\frac{\partial f}{\partial \sigma}\right\}^T\{d\sigma\}}{\left\{\frac{\partial f}{\partial \sigma}\right\}^T\left\{\frac{\partial f}{\partial \sigma}\right\}} \tag{8}$$

Constitutive Equation of Concrete: The stress vs. strain relation in elastic range is represented incrementally by the Hooke's law.

$$\{d\sigma\} = [D^e]\{d\varepsilon^e\} \qquad (9)$$

Then from Eq. 3 through Eq. 9 the constitutive equation in plastic range is represented by

$$\{d\sigma\} = [D^p]\{d\varepsilon\}$$

$$= \left[[D^e] - \frac{[D^e]\left\{\frac{\partial f}{\partial \sigma}\right\}\left\{\frac{\partial f}{\partial \sigma}\right\}^T [D^e]}{c\left\{\frac{\partial f}{\partial \sigma}\right\}^T \left\{\frac{\partial f}{\partial \sigma}\right\} + \left\{\frac{\partial f}{\partial \sigma}\right\}^T [D^e]\left\{\frac{\partial f}{\partial \sigma}\right\}} \right] \{d\varepsilon\} \qquad (10)$$

2) Tensile Side

When the maximum principal stress reaches the tensile strength, the cracking is assumed to occur along a plane normal to the principal stress direction. Accordingly, the stresses in the direction drop to zero. Cracking is judged at each Gaussian point, where three cracks can occur and they are mutually orthogonal. After cracking the shear transfer factor along the cracked surface is reduced to be 0.5. In case of repeated loading when the strain returns to point B in Fig. 2 (where the crack occured in the former stage), the concrete revives elasticity.

Modeling of Cover Concrete, Steel and Bond Elements

Cover Concrete: It is represented by a rod element possessing only longitudinal stiffness. The stress vs. strain relation is characterized by the uniaxial state of concrete. The reduction of strength after the peak stress is considered as shown in Fig. 2.

Steel Reinforcement: It is represented by a rod element possessing only axial stiffness. The stress vs. strain relation is assumed to be a bi-linear loop.

Bonds: They are modeled as a set of link elements connecting steel elements and concrete elements. Their bond vs. slip relation is assumed to be a slip-type bi-linear loop (Fig. 6).

EXPERIMENT AND ANALYSIS TO DETERMINE α

Outline of Experiment

The test specimen is a column with square hoops which is 45 cm long and cross sectional dimensions of 18cm x 18cm (Fig. 7). The diameter of hoops is 9 mm and their spacing is 20 mm. The measured vertical strain of concrete and strain of hoops are shown in Fig. 8 and Fig. 9 respectively. In these figures the solid lines are observed results at inside and outside, and the broken lines are their mean values excluding bending component.

Model for Analysis

In Fig. 10 the model for analysis is presented. Taking advantage of the symmetrical condition one quarter portion was considered horizontally. Vertically five layers were adopted to decrease the influence of boundary conditions. Material properties used in this analysis are presented in Fig. 11. The parameter $3/2\alpha$ of concrete is assumed to be 0, 0.1, 0.2, 0.3 and 0.4.

Results of Analysis

Loads vs. vertical strain of concrete is presented in Fig. 12. Here (A) shows the bearing forces of core concrete and cover concrete respectively. From this it is recognized that core concrete can sustain further force after the force of cover concrete has decreased as α increases due to the confinement effect of the hoops. In (B) the sum of the two values are compared with observed results. Loads vs. strain of hoop is presented in Fig. 13. From this the effectiveness of hoops is recognized distinctly after the stress of concrete has reached the vicinity of compressive strength of plain concrete. Among these results the value obtained by assuming $3/2\alpha=0.2$ shows the best agreement.

ANALYSIS OF COLUMN UNDER REPEATED LATERAL FORCES

Outline of Experiment

The test specimen is a 1/2 scaled column subjected to repeated lateral forces with a constant axial force which is equal to one third of compressive strength as shown in Fig. 14 (3). During the first and second cycles, the loading was gradually increased up to 30 tons and 60 tons respectively. Then 30 cycles of loading were applied to the specimen, keeping the maximum deflection constant at a relative deflection angle R of 1/100 rad. Finally, the relative deflection angle of the specimen was increased to 1/50 rad.

Model for Analysis

Analysis was performed on a half model by considering its antisymmetry (Fig. 15). The assumed material properties are shown in Tab. 1. Here, $3/2\alpha= 0.2$ is assumed from the result of the afore-mentioned preliminary study. The second and third loading cycles were simulated because the first one may be considered elastic.

Results of Analysis

Among obtained results deflection and strain of longitudinal reinforcement are shown in Fig. 16 and Fig. 17 respectively. Here the second and third cycle are separately shown.

The observed results are well simulated by this analysis from the positive to the negative region on the deflection and strain of longitudinal reinforcement. Especially, it is very important that the behavior while unloading is obtained by this incremental analysis method.

CONCLUSION

The nonlinear behavior of reinforced concrete columns were studied by 3-dimensional Finite Element Method developed by the authors. First the preliminary study determined the parameter α used in plastic condition of concrete. Then, on the basis of these results, a simulation analysis of a hooped column under repeated lateral forces was performed from the positive to the negative region and good agreement was obtained.

ACKNOWLEDGEMENTS

The authors wish to express their appreciation to Professor Emeritus K. Muto for his kind guidance. Y. Abe conducted the uniaxial test and S. Bessho provided the results of a hooped column. They are acknowledged with gratitude.

REFERENCES

(1) Darwin, D., and Pecknold, D.A., 1974, "Inelastic Model for Cyclic Biaxial Loading of Reinforced Concrete," University of Illinois

(2) Franklin, H.A., 1970, "Nonlinear Analysis of Reinforced Concrete Frames and Panels," Structures and Materials Research Department of Civil Engineering, University of California

(3) Hisada, T., Ohmori, N., and Bessho, S., 1972, "Earthquake Design Considerations in Reinforced Concrete Columns," The Journal of the International Association for Earthquake Engineering, Vol. 1, No. 1, pp.79-91

(4) Ngo, D., and Scordelis, A.C., 1967, "Finite Element Analysis of Reinforced Concrete Beams," ACI Journal, Vol. 64, No.3, pp.152-163

(5) Suidan, M., and Schnobrich, W.C., 1973, "Finite Element Analysis of Reinforced Concrete," Journal of the Structural Division, ASCE, Vol. 99, pp.2109-2122

(6) Ziegler, H., 1959, "Modification of Prager's Hardening Rule", Quart., Appl. Math., Vol. 17, No.1, pp.56-65

(7) Zienkiewicz, O.C., 1971, "The Finite Element Method in Engineering Science," McGraw-Hill

TAB. 1 MATERIAL PROPERTIES

Concrete

compressive strength	370 kg/cm²
elastic limit	133 kg/cm²
tensile strength	28 kg/cm²
elastic modulus	180 t/cm²
semi-elastic modulus	136 t/cm²
$3/2\alpha$	0.2
Poisson's ratio	0.2
limiting comp. strain	0.0035

Steel

yield stress	
longitudinal bar	3.7 t/cm²
transverse bar	3.6 t/cm²
Young's modulus	2100 t/cm²

Bond

yield stress	
longitudinal bar	50 kg/cm²
transverse bar	30 kg/cm²
first stiffness	25 t/cm³
second stiffness	0.84 t/cm³

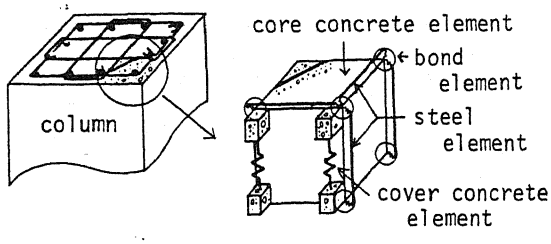

FIG. 1 MODELING OF COLUMN

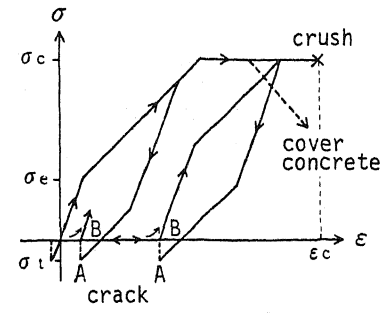

FIG. 2 HYSTERETIC LOOP OF CONCRETE

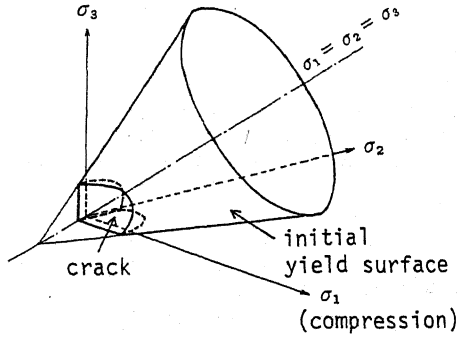

(A) 3 DIMENSION

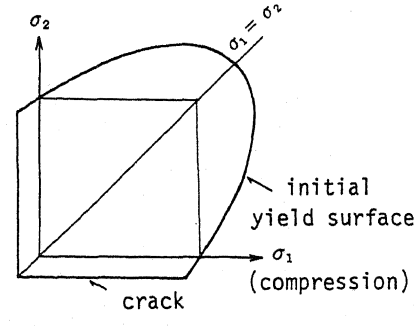

(B) 2 DIMENSION

FIG. 3 INITIAL YIELD CONDITION

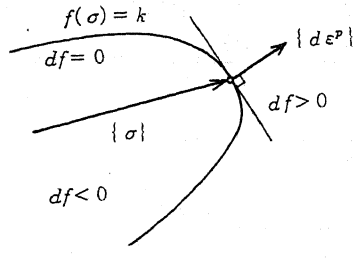

FIG. 4 FLOW RULE

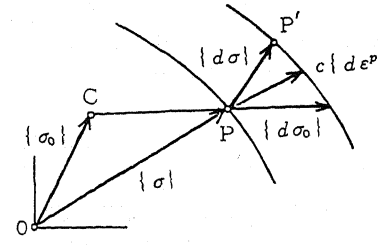

FIG. 5 HARDENING RULE

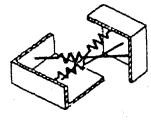

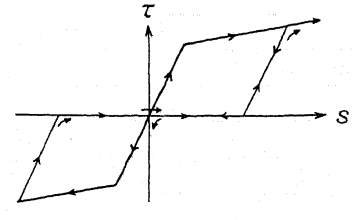

FIG. 6 HYSTERETIC LOOP OF BOND

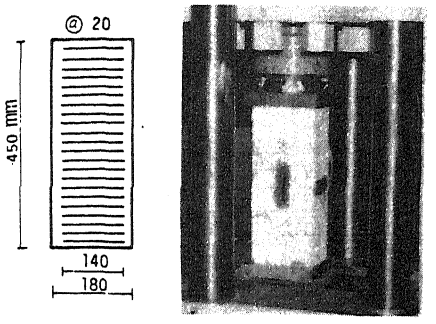

FIG. 7 TEST SPECIMEN

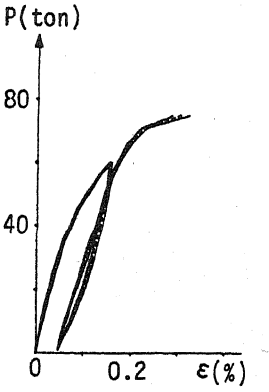

FIG. 8 MEASURED STRAIN OF CONCRETE

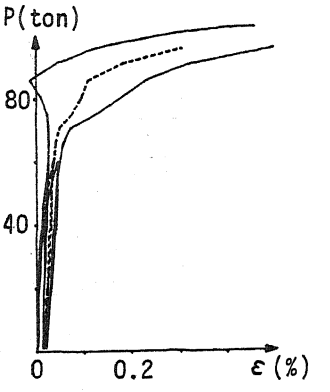

FIG. 9 MEASURED STRAIN OF HOOP

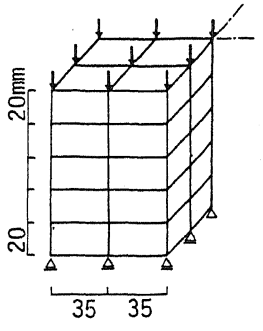

FIG. 10 MODEL FOR ANALYSIS

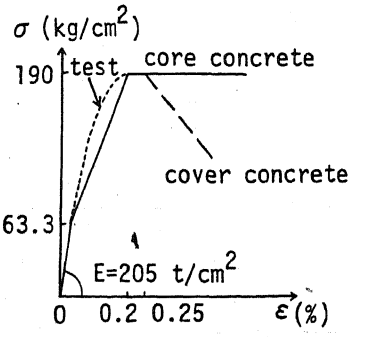

(A) CONCRETE

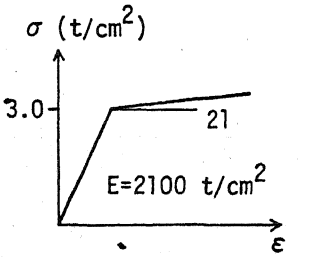

(B) STEEL

FIG. 11 MATERIAL PROPERTIES

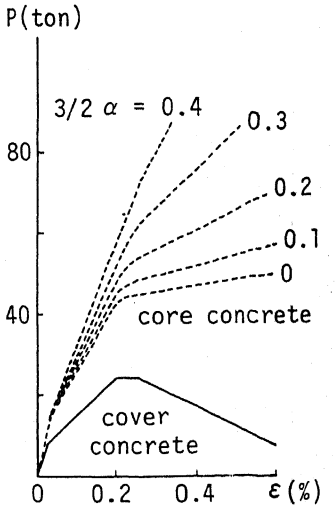

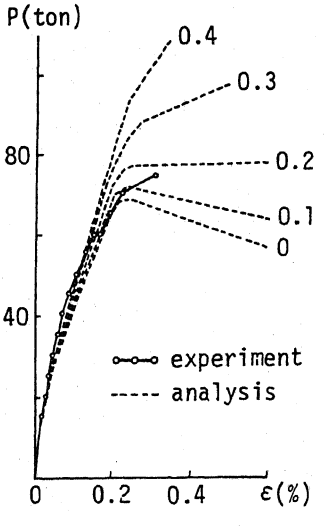

(A) CORE AND COVER CONCRETE (B) TOTAL

FIG. 12 LOADS vs. VERTICAL STRAIN OF CONCRETE

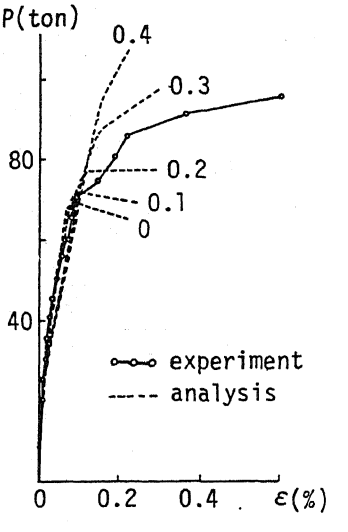

FIG. 13 LOADS vs. STRAIN OF HOOP

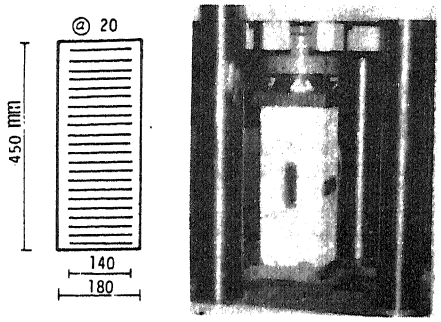

FIG. 7 TEST SPECIMEN

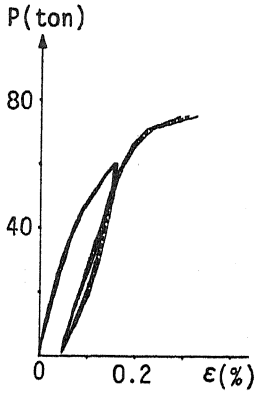

FIG. 8 MEASURED STRAIN OF CONCRETE

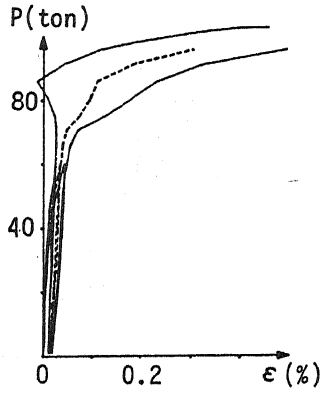

FIG. 9 MEASURED STRAIN OF HOOP

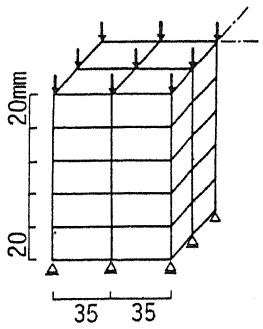

FIG. 10 MODEL FOR ANALYSIS

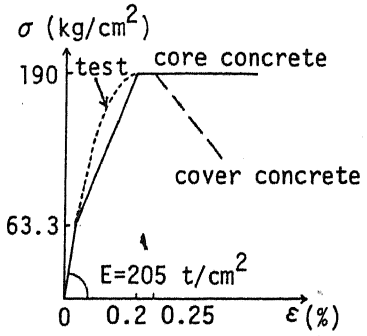

(A) CONCRETE

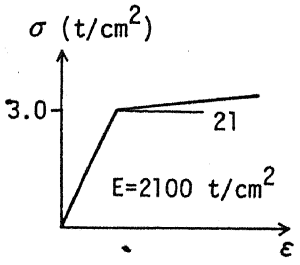

(B) STEEL

FIG. 11 MATERIAL PROPERTIES

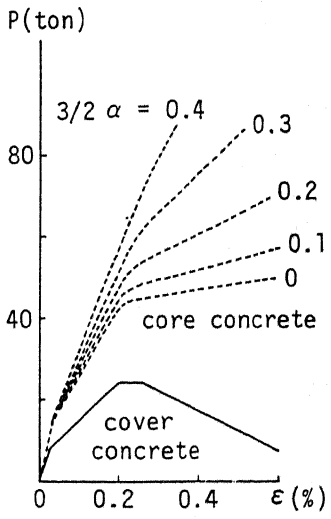

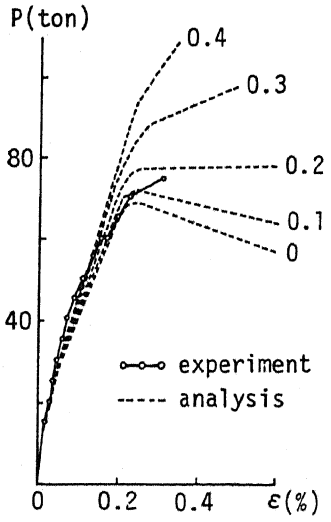

(A) CORE AND COVER CONCRETE (B) TOTAL

FIG. 12 LOADS vs. VERTICAL STRAIN OF CONCRETE

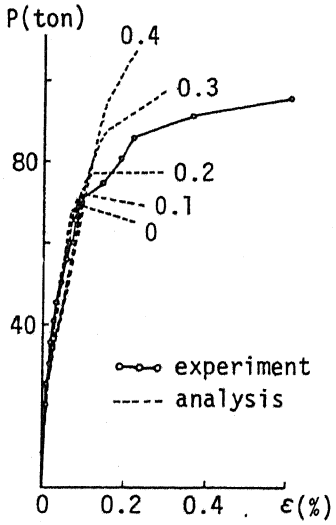

FIG. 13 LOADS vs. STRAIN OF HOOP

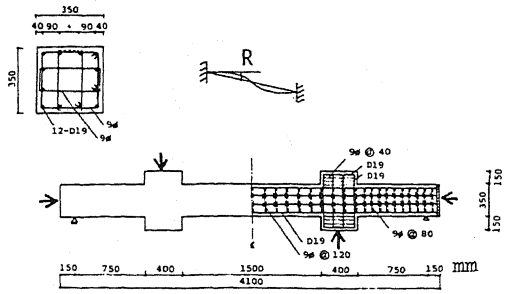

FIG. 14 TEST COLUMN

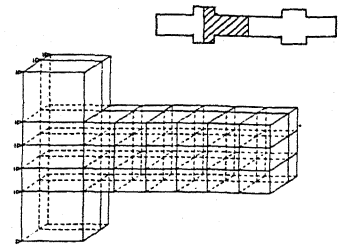

FIG. 15 MODEL FOR ANALYSIS

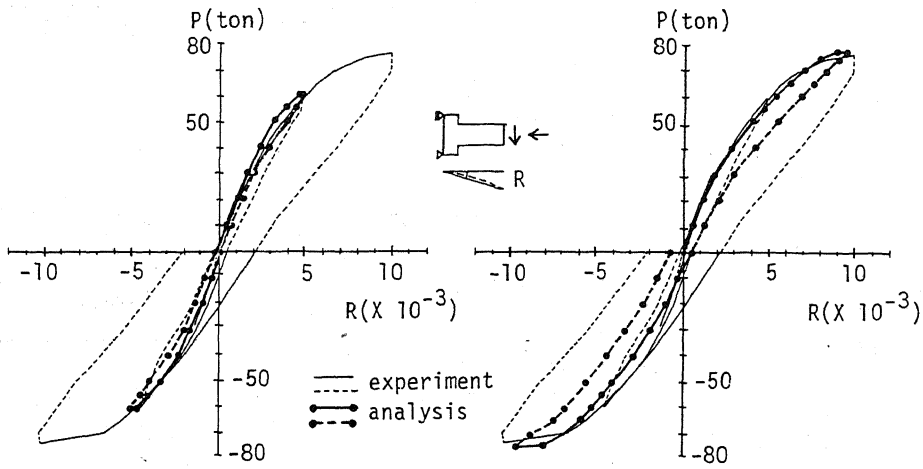

(A) 2nd CYCLE (B) 3rd CYCLE

FIG. 16 RELATIVE DEFLECTION

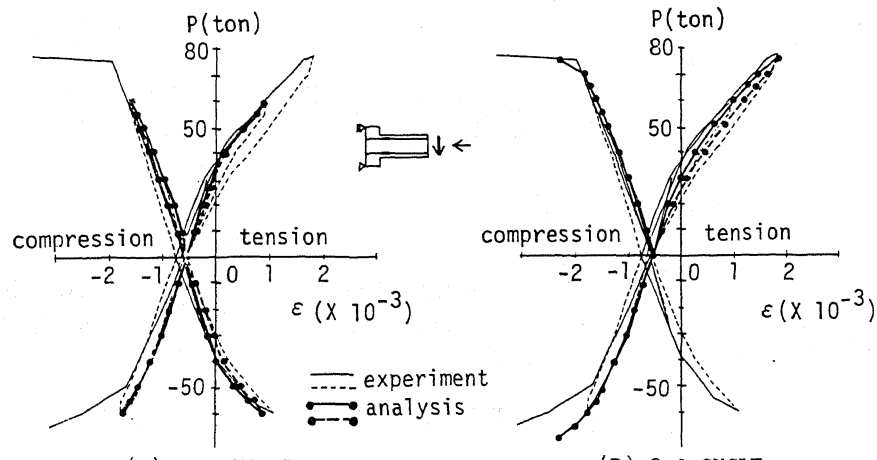

(A) 2nd CYCLE (B) 3rd CYCLE

FIG. 17 STRAIN OF LONGITUDINAL REINFORCEMENT